Integration and Testing of Ice-/Mixed-Phase Precipitation Models for GPM Radar-Radiometer Algorithm Applications

William Olson[1], Kwo-Sen Kuo[2], Mircea Grecu[3], Benjamin Johnson[4], Robert Schrom[5], Craig Pelissier[6], Adrian Loftus[2], Stephen Munchak[7]

1: Joint Center for Earth Systems Technology/Univ. Maryland Baltimore County; 2: Earth System Science Interdisciplinary Center/Univ. Maryland College Park; 3: Goddard Earth Sciences Technology and Research/Morgan State University; 4: University Corporation for Atmospheric Research; 5: Universities Space Research Association; 6: Science Systems and Applications, Inc.; 7: NASA/Goddard Space Flight Center

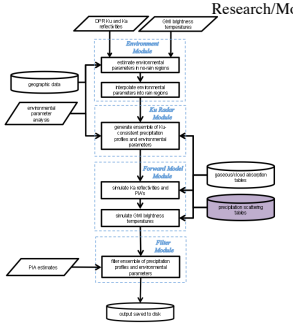

Why? **to improve the physical / statistical models used in GPM radar and combined radar-radiometer precipitation estimation algorithms.** At left is a schematic of the GPM combined radar-radiometer precipitation estimation algorithm. This algorithm uses input radar reflectivities from the Dual-frequency Precipitation Radar (DPR) and microwave radiances from the GPM Microwave Imager (GMI) to deduce profiles of precipitation in all phases (liquid, ice, and mixed-phase). The accuracy of these precipitation estimates depends not only on the validity of the input data, but also on the realism and representativeness of the physically-based precipitation profile models used to fit the input data.

In the figure at left, the microwave electromagnetic scattering properties of precipitation particles are tabulated in the purple static file. These tabulated scattering properties are functions of the assumed particle phase (temperature), size distribution, density distribution (for ice and mixed-phase), habit, and meltwater fraction. In addition to the tabulated scattering properties, for algorithm applications it is also important to prescribe the statistical behavior of precipitation particle size distributions; e.g., the covariance of particle size distribution parameters as a function of altitude. In sum, the objective of this work is to develop better parameterizations of the physical and statistical properties of ice and mixed-phase precipitation for algorithm applications.

Modeling of Ice-/Mixed-Phase Precipitation in Algorithms

The particle scattering models developed during the TRMM era assumed that all precipitation-sized particles were spherical, due to the simplicity of computing the single-scattering properties of spherical particles. However, it is known that larger raindrops are better approximated by oblate spheroids, and ice-phase precipitation particles exhibit a variety of complicated particle shapes. The focus of our investigation will be to see if we can find reasonable parameterizations of ice- and mixed-phase precipitation particle size distributions and particle shapes that produce bulk scattering properties that are consistent with simultaneous radar, radiometer, and *in situ* microphysics probe observations from the GPM field campaigns.

For each particle size in any prescribed particle size distribution, the mass (or density) of the particle, its shape or habit, and the meltwater fraction of the particle must be specified. Starting with pure ice-phase precipitation, we have examined the properties of both pristine crystals (plates, needles, dendrites) as well as aggregates of crystals. Aggregate ice particles are particularly important because they tend to be the dominant particle habit among particles of relatively large size, and they also produce high radar reflectivities at the onset of melting.

We have implemented a 3-D growth model for pristine crystals and a pseudo-gravitational collection model to create aggregate particles. The figure at above right contains images of pristine ice crystals that were simulated using the growth model, and the various aggregates shown below the crystals are constructed from crystals of the same habit but with different sizes and spatial orientations, that have been sequentially collected. The constructed particles are filtered to represent different observed mass-size relations.

Using this method, roughly 6600 ice particles have been simulated, ranging from single pristine crystals to multi-crystal aggregates (sizes from 260 to 14,260 μm maximum dimension, although recently, particles with maximum dimensions up to ~25,000 μm have been generated). Each ice particle is constructed on a 3D numerical grid, and the microwave single-scattering properties of each particle are computed using the discrete dipole approximation (DDA; see Draine and Flatau, JOSA, 1994). In the DDA, a particle is represented by a grid of dipoles; each dipole interacts with an incoming electromagnetic wave as well as the scattered waves from all other dipoles in the particle. At above right are simulations of the single-scattering parameters of the individual particles (blue dots) using DDA, as well as the parameters for spheres of the same mass and either variable density (solid green lines) or a constant density of 0.1 g cm^{-3} (dashed green lines), derived from Mie theory.

Relative to the variable-density spheres, the constant density Mie spheres provide a better approximation to the aggregate particle backscatter efficiencies at 13.6 and 35.5 GHz. However, note that at the 89 and 165.5 GHz channel frequencies of the GMI, the asymmetry parameters of the Mie spheres are consistently higher than the aggregate asymmetry parameters. This characteristic leads to an inability of Mie spheres to simultaneously fit radar and high-frequency radiometer data in field campaign tests (see Olson et al., JAMC, 2016).

The properties of melting ice crystals, aggregates, and graupel are also being investigated. In one approach, the ice precipitation is represented on a 3D grid, and melting occurs based upon the exposure of ice to air (warming), while meltwater migrates toward local centers of mass to simulate the effects of surface tension. The evolution of a melting aggregate based upon this approach is shown at above right, with ice in blue and meltwater in red. The single-scattering properties of the melting aggregates are computed using DDA and "mapped" to spherical particles with the same mass and meltwater fraction in simplified 1D thermodynamic simulations of the melting layer. Simulations of bulk reflectivity and specific attenuation based upon polydispersions of melting particles are shown at right, for different initial median volume (liquid-equivalent) diameters. It is evident that polydispersions of melting homogeneous spheres (0.1 g cm^{-3}, solid lines) have properties that are different from those of melting nonspherical aggregates (dashed lines). The different attenuation-reflectivity relationships represented by these melting particles will impact combined radar-radiometer estimates of precipitation profiles.

simulated crystals/aggregates and their single-scattering properties

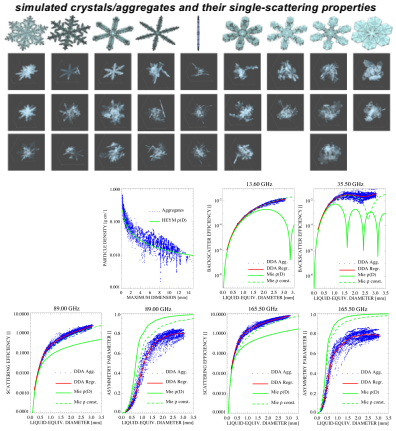

simulated melting aggregates

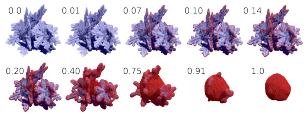

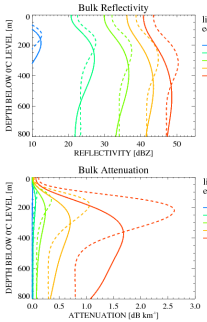

Impact of Nonspherical Ice Model on the GPM Combined Algorithm

The nonspherical ice-phase precipitation model (aggregates) described at left was used to generate polydispersions of "snow" particles, and the scattering properties of these particles were integrated over assumed normalized gamma particle size distributions to obtain bulk scattering properties. These scattering properties were introduced into look-up tables that support the V05 and prototype V06 combined radar-radiometer precipitation estimation algorithms.

GPM combined algorithm estimates of snow rates just above the freezing level, as well as simulated upwelling brightness temperatures at 89, 166, and 183±7 GHz based upon the spherical ice-particle model (Mie 100, for 0.1 g cm^{-3} constant density spheres) and the nonspherical ice particle model (KuoSno, V05) are shown, for overpasses of mesoscale convective systems on orbits #2901 (top 3 rows) and #6206 (bottom 3 rows). Also shown are the GMI observed brightness temperatures at 89, 166, and 183±7 GHz in the lowest row of each set. The introduction of nonspherical snow into the combined algorithm results in lower estimated snow rates, yet the simulated scattering signatures (brightness temperature depressions) at the higher microwave frequencies are greater, in better agreement with the GMI scattering signatures. This is primarily due to the lower asymmetry parameters of the nonspherical snow, which results in greater backscatter of low-intensity cosmic background radiances from space.

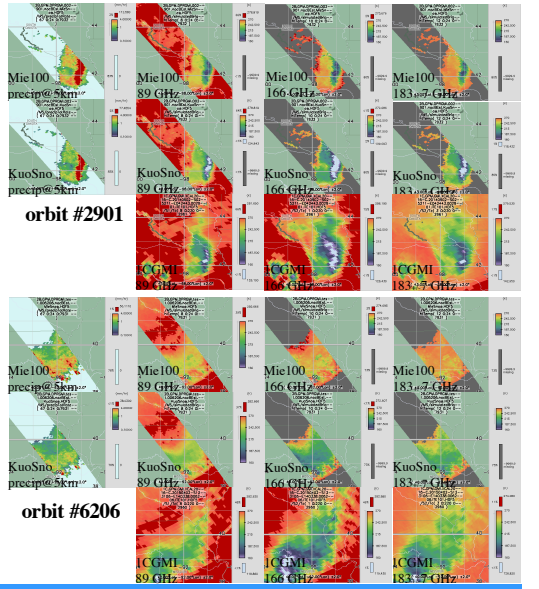

Below are 2-D histograms of simulated vs. observed 166 GHz brightness temperatures, derived from combined algorithm applications using spherical snow (at left) and nonspherical snow (at right) models, over the month of September, 2014. Note that the more realistic scattering of the nonspherical snow model results in lower simulated brightness temperatures, in agreement with GMI observations. The better fidelity of simulated brightness temperatures is important, because the higher-frequency microwave channels can now be used with more confidence in the estimation of snow rates. Also, the estimated precipitation profiles and associated brightness temperatures can now be introduced into the radiometer algorithm databases to support Bayesian estimation with less bias.

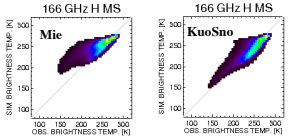

Single-Scattering Properties of Melting, Nonspherical Ice

Calculation of the microwave scattering properties of melting nonspherical (aggregate) ice particles is a particular challenge. Simple ice particle melting algorithms that convert ice to meltwater on a fixed grid do not conserve mass properly, as liquid water has a higher density than ice and therefore occupies a smaller volume. In addition, there is the general problem of limiting the number of particle dipoles to a quantity that is computationally feasible for DDA.

To address these issues, a new particle property spatial compositing (blurring) algorithm is being explored. At right are the 94 GHz absorption and scattering cross sections calculated using DDA of a 2.6 mm liquid equivalent diameter ice particle with 10% meltwater, plotted as functions of particle orientation. The top panels are full-resolution DDA calculations, while the middle panels show the approximate DDA, where properties are blurred in 6 x 6 x 6 grid-box volumes. Mass is approximately conserved in the blurred particles, but the cross sections differ from the full-resolution calculations. Alternative approaches, including local refractive index mixing, are also under consideration.

from Rob Schrom